Deformation-induced ambient temperature α-to-β phase transition and nanocrystallization in (α + β) titanium alloy

Yong Han[a] and Huaye Zhuang
State-Key Laboratory for Mechanical Behavior of Materials, Xi'an Jiaotong University, Xi'an 710049, China

Jian Lu
Department of Mechanical Engineering, The Hong Kong Polytechnic University, Hung Kom, Kowloon, Hong Kong, China

(Received 12 March 2009; accepted 10 July 2009)

Ambient temperature α-to-β phase transition and nanocrystallization in the aged Ti–25Nb–3Mo–3Zr–2Sn titanium alloy was achieved by surface mechanical attrition treatment (SMAT). The phase transition occurs at α/β interfaces and extends to α phase interiors with increasing strain. It is irreversible and diffusion controlled. The stress-induced increase of Gibbs energy and enrichment of Nb may cause a high order of lattice instability of the α phase adjacent to the α/β interfaces and compel the α phase to β phase. The presence of fine α needles in the aged alloy and the phase transition from α to β with increasing strain are viewed to play a crucial role in the subsequent nanostructuring.

I. INTRODUCTION

Solid-state phase transition may provide an effective way to modify structure; thereby, the phase transition in titanium and its alloys has been studied extensively in theory and experiment. Pure titanium crystallizes in a hexagonal close packed (hcp, α) structure at ambient temperature and pressure but transforms to a body-centered cubic (bcc, β) phase at high temperature. At high pressure and ambient temperature, titanium undergoes a series of allotropic transitions (α→ω→γ→δ) with increasing pressure,[1–6] in which the electronic transfer between the broad sp-band and the narrow d-band is the driving force for the phase transitions. For example, the phase transition from α to ω (another hexagonal structure with three atoms per unit cell) is observed at >2 GPa.[1–3] The ω phase remains stable up to 116 GPa, at which point a structural phase transition to an orthorhombic (γ) phase is observed,[5] followed by another orthorhombic (δ) phase reported to exist at >140 GPa and to be stable up to 220 GPa.[6] It is found that the ω-to-α, γ-to-ω, and δ-to-γ processes are reversible on pressure release.[3,6] The high-pressure β phase has not been observed in pure titanium in most of the experiments,[4] except as claimed by Ahuja et al.[7] for the observation of the ω-to-β transition in the range 40–80 GPa. In addition to high pressure studies, shock[8,9] and severe plastic deformation[10] experiments performed at ambient temperature only show the α-to-ω phase transformation in Ti and Ti–6Al–4V alloy. Also, complete transformation and significant refinement from the coarse-grained α-Zr to ω-phase occurs during high-pressure torsion, and the nanocrystalline ω-Zr phase is stable at room temperature and pressure.[11]

Compared with α and (α + β) titanium alloys, β-titanium exhibits relatively lower elastic modulus, superplasticity and ductility, and better formability.[12,13] Considerable efforts have been devoted to exploring novel β-titanium alloys by addition of d-electron–rich elements such as Mo and Nb to stabilize β phase at low temperature.[12,14] In α or (α + β) titanium alloys, thus far, the transformed β phase from the α phase has not been found in most of the ambient temperature experiments, except a recent report showing a high pressure (>67 GPa)–induced α-to-β phase transition in an aged Ti–15Mo–3Nb–3Al–0.2Si alloy.[15] However, why and how this phase transition takes place have not been studied.[15]

Because of unique physical, mechanical, and biological properties of nanostructured materials relative to coarse-grained counterparts,[16,17] the feasibility of producing nanostructured β-titanium alloys by deformation has attracted many concerns. β-titanium alloys with an Mo equivalent (Mo_{eq}) >10 wt% exhibit a high stability against martensitic transformation during deformation.[18,19] The deformation behavior of β-titanium alloys strongly depends on the stability of the β phase; with decreasing β phase stability, the deformation mechanism changes from slip to deformation twinning and/or martensitic transformation.[20,21] On severe plastic deformation (SPD), nanostructuring occurred more easily in the less-stabilized β-titanium alloys such as the Ti–Nb–Ta–In

[a]Address all correspondence to this author.
e-mail: yonghan@mail.xjtu.edu.cn
DOI: 10.1557/JMR.2009.0420

alloy with a low Mo equivalent (Mo_{eq}) of 8.6 wt%,[21] and Ti–24Nb–4Zr–7.9Sn (wt%),[22] however, could not be achieved in the more stabilized Ti–Nb–Ta–Cr alloy with Mo_{eq} as high as 18 wt% because of the lack of assistance from β-to-α" martensitic transformation.[21] Although stress-induced martensitic transformation accelerates grain refinement during plastic deformation, it results in serious damage to recoverable elasticity and ductility of severely cold-rolled multifunctional titanium alloys.[23]

In this study, a direct α-to-β phase transition at ambient temperature was achieved in aged TLM titanium alloy (stabilized as a mixture of α + β phases) by surface mechanical attrition treatment (SMAT), and the mechanism of the phase transformation and its role in nanostructuring of the alloy were explored.

II. EXPERIMENTAL PROCEDURE

The used titanium alloy, TLM, has a composition of Ti–25Nb–3Mo–3Zr–2Sn (wt%) with Mo_{eq} of 9.9 wt% and β transition temperature of 710–720 °C.[24] It was solution-treated at 750 °C for 1 h, cooled in air, and aged at 550 °C for 6 h. Three samples of the aged TLM (100 mm in diameter and 5 mm in thickness) were mounted in a vacuum chamber of SNC-I surface mechanical attrition treatment set-up as schematically described elsewhere,[25] and impacted by flying zirconia balls (2 mm in diameter, resonated by a vibration generator at frequency of 50 Hz) at room temperature for 5, 15, and 30 min, respectively. As a comparison, one sample of the solution-treated TLM was SMARed under the same condition for 30 min. The phase components of the as-aged sample and the SMATed samples were analyzed by X'Pert PRO x-ray diffraction (XRD; PANalytical, Almelo, The Netherlands) in θ-2θ geometry using Cu-K_α rays. Transmission electron microscopy (TEM) observations of the layers at different depths beneath the 30-min SMATed sample surface were performed using a JEM-2100F field emission microscope (JEOL, Tokyo, Japan) operating at 200 kV. Analysis of elemental composition profiles across the α phase was carried out by energy dispersive x-ray spectrometer (EDX) under STEM nanoprobe conditions on the JEM-2100F field emission microscope. An electron probe of ~1 nm makes it possible to measure directly elemental composition across the nanoscale region.[26] To understand the thermal stability of the SMATed TLM, the specimens cut from the 30-min SMATed plate were encapsulated in quarts tubes with vacuum of 7×10^{-4} Pa to receive annealing treatment at 200, 300, and 400 °C for 6 h, respectively, and XRD analyses were performed.

III. RESULTS

TEM and XRD analyses show that the aged TLM consists of (α + β) two-phase microstructure with an α phase of ~31%. The α phase exhibits a needle-like shape in white color, having a clear straight interface with the adjacent β-phase matrix [Fig. 1(a)]. In the aged TLM, EDX-detected Nb distributes homogeneously over the α phase and β phase with contents of 3.92 and 27.02 at.%, respectively. After SMAT of the aged TLM, however, the XRD intensities of the α phase significantly decrease with prolonging treatment time [Fig. 1(b)]; especially for the 30-min SMATed sample, only diffraction peaks attributed to β phase are visible, suggesting that the x-rays detected outmost layer of the sample consists of single β phase. It is also noticeable that the diffraction peaks of the β phase are apparently broadened after SMAT, indicating that the grains in the XRD-detected layer are refined.

As known, the repeated multidirectional impacts at high strain rates onto the sample surface during SMAT result in

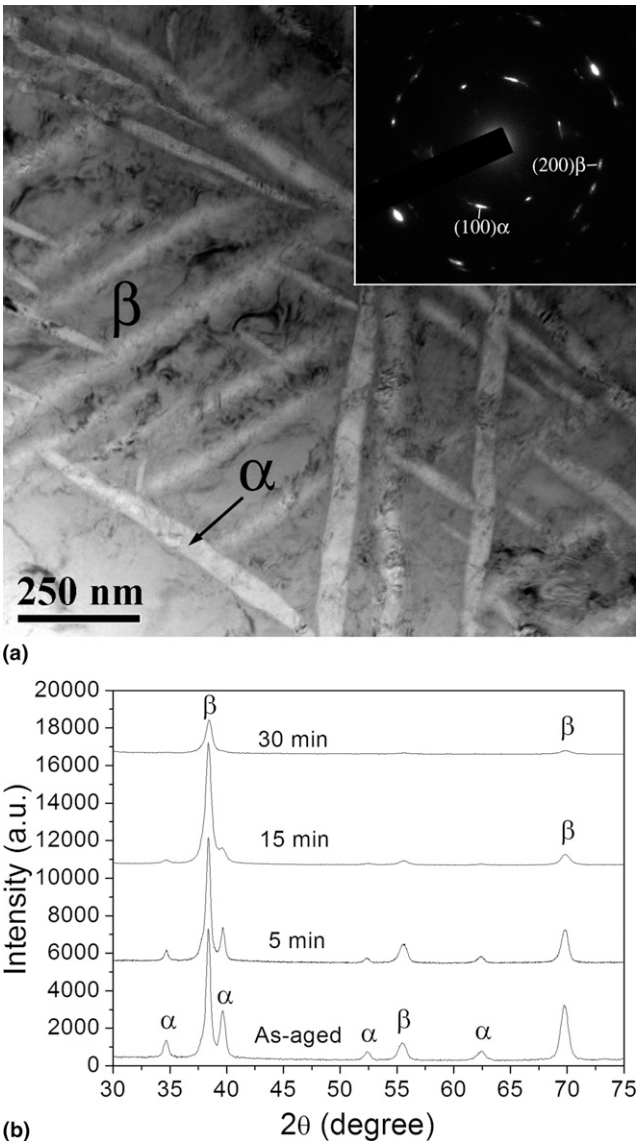

FIG. 1. (a) TEM image of the as-aged TLM sample. (b) XRD patterns of the aged TLM samples subjected to SMAT for 5, 15, and 30 min.

severe plastic deformation and gradient variation of strain from the treated top surface (large) to the deep matrix (essentially zero).[25] Figure 2 shows TEM images taken from the layers at depths of 60, 30, and 15 μm beneath the surface of the 30-min SMATed sample. In the 60-μm-deep layer, the high density of dislocations is visible in the β-phase matrix and accumulates in front of the α/β interfaces, indicating that severe plastic deformation occurs in the layer. Compared with the as-aged state shown in Fig. 1(a), the α needles in the layer at depth of 30 μm beneath the surface are narrowed, and some α/β interfaces are curved toward α needles [Fig. 2(b)]. It is clear that the α needles in the layer at depth of 15 μm beneath the surface become small in both size and amount [Fig. 2(c)]; also, the EDX-detected content of Nb distributes heterogeneously in the α needles of this layer, increasing from 6.98 at.% detected at the center to 10.63 at.% near the α/β interface [Fig. 2(d)], which is higher than that in the as-aged α phase (3.92 at.%). This result indicates that the diffusion of Nb toward α phase and thereby compositional change happened in the deformed layers during SMAT.

The α needles in the top surface layer of the 30-min SMATed sample are invisible [Fig. 3(a)], and the layer consists of single β phase as confirmed by selected-area electron diffraction (SAED) pattern [inset of Fig. 3(a)]. On the other hand, the continuous ring characteristics of the SAED pattern in the inset of Fig. 3(a) shows that the top surface is nanostructured, with a grain size of ~20–30 nm as further confirmed by a high-resolution TEM (HRTEM) image [Fig. 3(b)]. The structural evolution of the layers with depth indicates that the phase transition from α to β indeed occurs and is irreversible in nature. Furthermore, it is important to note that any XRD peak and SAED spot that could not be assigned to α or β phase have not been observed, suggesting that α phase in the aged TLM can directly transform to β phase at ambient temperature under impact loading.

To understand how the α phase transforms to the β phase during SMAT, the HRTEM image of the area around α/β interface, taken from the layer at depth of 60 μm beneath the 30-min SMATed sample surface, is shown in Fig. 4(a), in which the concerned squares

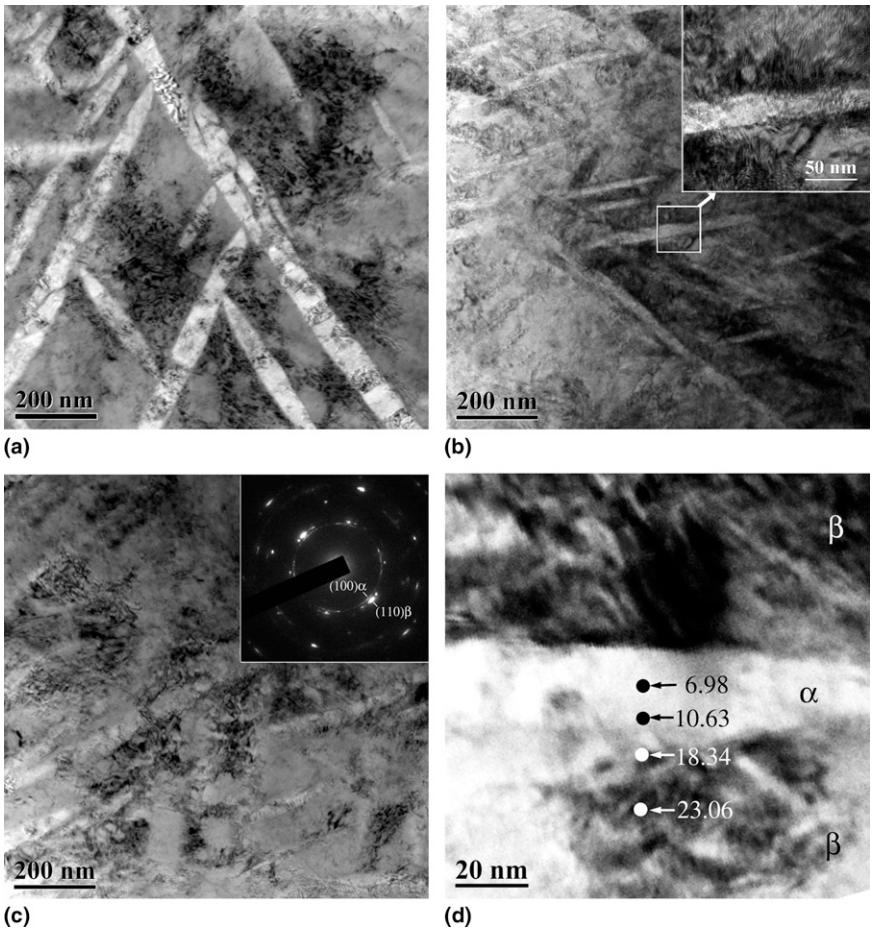

FIG. 2. TEM images taken from the layers at depths of (a) 60, (b) 30, and (c) 15 μm beneath the surface of the 30-min SMATed sample; inset in (b) shows a magnified view of a curved α/β boundary. (d) STEM image showing EDX-detected Nb content (marked in the image, at.%) in the α and β phases of the 15-μm deep layer.

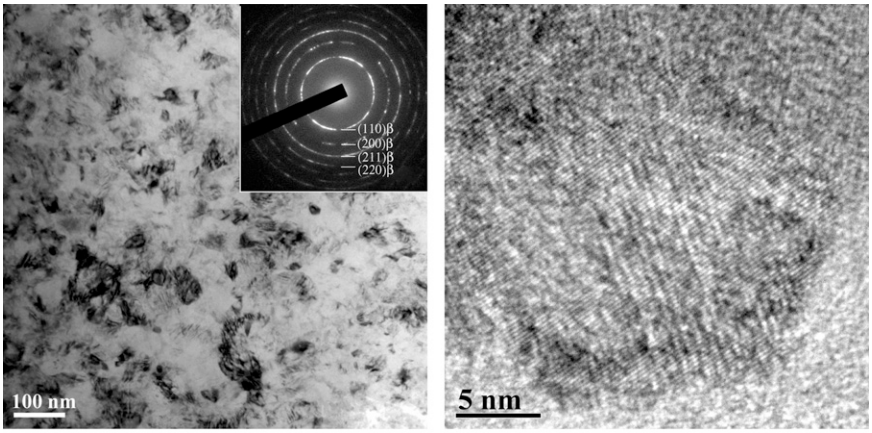

FIG. 3. TEM images taken from the top layer of the 30-min SMATed sample: (a) bright-field image and SAED pattern (inset) and (b) HRTEM image.

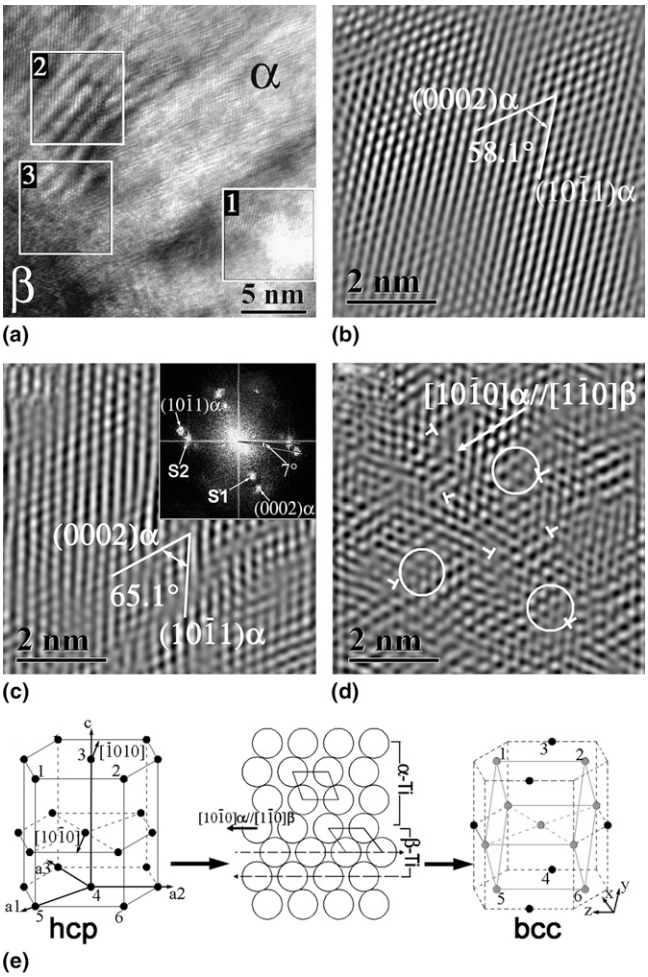

FIG. 4. (a) HRTEM image of the area around α/β boundary, taken from the layer at depth of 60 μm beneath the 30-min SMATed sample surface. (b) Inverse FFT image of square 1 marked in (a). (c) Inverse FFT and FFT (inset) of square 2 marked in (a). (d) Inverse FFT of square 3 marked in (a). (e) Schematic of the α-to-β phase transition, showing lattice correspondence between the transited β phase and the parent α phase.

marked 3, 2, and 1 are inside the α phase and are gradually further from the α/β interface. In square 1, the (0002) and (10−11) planes of the α phase have a normal spacing of 0.234 and 0.224 nm, respectively, showing an angle of 58.1 degrees between the two planes [Fig. 4(b)]. A fast Fourier transformation (FFT) of the square 2 [inset of Fig. 4(c)] exhibits clear diffraction spots of undeformed $(0002)_\alpha$ along with its deformed one (shown as S1) and undeformed $(10-11)_\alpha$ along with its deformed one (shown as S2). It is indicated that the spacing of partial $(0002)_\alpha$ planes in square 2 increase to 0.339 nm (corresponding to S1), suggesting an elongation of the hcp structure of α phase along the [0001] direction. As a consequence of the elongation, partial $(10-11)_\alpha$ planes (corresponding to S2) in square 2 is rationed ∼7° relative to the undeformed (10−11), resulting in the increase of the angle between the deformed $(10-11)_\alpha$ and undeformed $(0002)_\alpha$ planes to 65.1°, and at the same time, the increase in spacing of the $(10-11)_\alpha$ planes to 0.255 nm is visible [Fig. 4(c)]. The aforementioned lattice spacing changes of the deformed $(0002)_\alpha$ and $(10-11)_\alpha$ planes might be attributable to the compositional change in α-Ti during SMAT. The magnified inverse FFT image of square 3 [Fig. 4(d)] shows that the α-phase lattice is more severely distorted, and many dislocations and stacking faults are visible in this square. More importantly, the nuclei with bcc-like structure, which consist of three to four atomic layers, can be found in some of the severely distorted fine-scale regions as marked by white circles. Each of the nuclei is formed by a shift of atoms on $(0002)_\alpha$ planes along the [10−10] or [−1010] direction to 0.085 nm, as schematically shown in Fig. 4(e).

Figure 5 shows XRD patterns of the 30-min SMATed samples after annealing at 200, 300, and 400 °C for 6 h. The XRD pattern of the 200 °C annealed sample is quite similar to that of the as-SMATed sample, only exhibiting diffraction peaks of the β phase. When annealed at

300 and 400 °C, diffraction peaks of the α phase appear at a 2θ of 34.9 and 39.7°, indicating that β-to-α transition happened during annealing at temperatures >300 °C. It is also suggested that the β phase (including untransited β-Ti and transited β-Ti from α-Ti during SMAT) in the SMATed sample is stable up to 300 °C. The changes of grain size, strain, and phase composition of the SMAT-induced nanocrystallized TLM alloy during annealing at 200 to 650 °C has been studied by us and will present elsewhere.

IV. DISCUSSION

A. α-To-β phase transition in the aged TLM alloy during SMAT

During SMAT, the temperature rise at the sample surface induced by the repeated impacts was as low as ~50–100 °C,[25] suggesting that the α-to-β phase transition in the aged TLM alloy during SMAT is not induced by temperature rise. On the other hand, hcp metals such as pure Ti[27] and Zr[28] did not undergo any phase transition during SMAT. We also examined the structure of the Ti–6Al–4V alloy STATed under the same condition as this work, and no α-to-β phase transition was found. These results indicate that the α-to-β phase transition in TML alloy induced by SMAT is alloying element dependent.

The structure of this alloy is many α needles embedding in a soft β phase. With an increasing degree of deformation (from the deep matrix to the top surface), dislocation slip becomes dominant. The α phase has a low-symmetry hcp structure, which lacks sufficient-independent slip systems,[27] thus making it difficult for slip dislocations that are activated in the β phase to pass through the α phase. Instead, slip dislocations in the β phase strongly interact with the partial dislocations of the α/β interface and accumulate at the interface [Fig. 2(a)], resulting in a large stress concentration at the interface and a stress gradient from the interface to the interior. Because the stress gradient could cause diffusional flow of a fast diffusing element,[29] Nb as a fast diffusing element would migrate from the α/β interfaces to the α phase interiors, resulting in enrichment of Nb [Fig. 2(d)] relative to that in the as-aged α phase. Also, the application of the high stress concentration to the α phase adjacent to the interface significantly increase its Gibbs free energy by several hundreds Joule per mol.[13] The increase of Gibbs free energy and the enrichment of Nb may eventually cause a high order of lattice instability of the α phase adjacent to the interface and compel the α phase to β phase. In combination with Figs. 2–4, it is indicates that the phase transition from α to β firstly occurs at the α/β interfaces, then extends to the interiors of α needles with increasing the strain. In the SMATed surface layer where subjects to the highest degree of deformation, the α phase completely transforms to β phase. It could be considered that the α-to-β phase transition in SMATed TML alloy is controlled by Nb diffusion which is caused by stress gradient, instead of diffusionless martensitic transformation happened in high pressure experiment of Mg.[30]

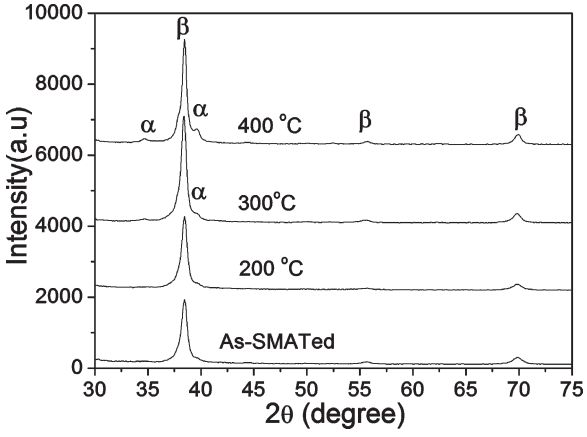

FIG. 5. XRD patterns of the 30-min SMATed samples after annealing at 200, 300, and 400 °C for 6 h.

B. Nanocrystallization induced by SMAT

This work indicated that SMAT can refine the surface grains of the aged alloy (composed of α and β phases) into nanoscale grains (Fig. 3). However, nanostructuring of the solution-treated alloy (consisted of single β phase) cannot be achieved under the same SMAT condition, as shown in Fig. 6. It shows that dislocations and deformation twins are visible; in addition, only the β phase could be identified from the SAED pattern (inset of Fig. 6),

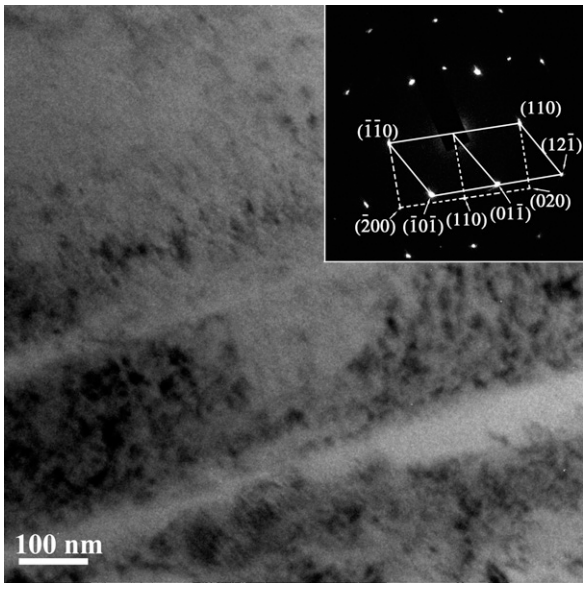

FIG. 6. TEM image taken from the surface layer of the solution-treated alloy after SMAT for 30 min; the inset shows that the gray bands in the image are twins.

without any other phases such as deformation-induced α" martensite observed in the Ti–Nb–Ta–In alloy.[21]

The aforementioned difference in the SMAT-induced nanostructuring ability of both the aged and solution-treated TLM samples is thought to be related to their microstructure. The aged TLM sample exhibits sandwich structure, consisting of the β phase and many fine α needles that divide the β matrix into discontinuous blocks [Fig. 1(a)]. It is well known that the dislocation slip is the dominant deformation mechanism of β-Ti. During SMAT of the aged TLM sample, the preexisting α needles have an hcp structure lack of sufficient independent slip systems,[27] thus making it difficult for slip dislocations that are activated in the β phase to pass through the α phase. Instead, slip dislocations in β phase strongly interact with the partial dislocations of the α/β interface and accumulate at the interface [Fig. 2(a)], simultaneously resulting in a stress concentration at the α/β interfaces and a stress gradient from the interfaces to the interior of α needles. With increasing degree of deformation (from the deep layer to the top surface layer), the accumulated dislocations would be enhanced, resulting in the formation of dislocation cells to further subdivide the sandwiched β-Ti region into refined blocks; at the same time, α phase gradually transforms to β phase [Figs. 2(b)–2(d)] because of the enhanced Nb diffusion. The α-to-β transition provides more slip systems and consequently accommodates the increasing strain, resulting in more severe plastic deformation of the upper layer and formation of nanostructured structure. Based on the evidence that the solution-treated TLM consists of single β phase and nanostructuring of the solution-treated alloy cannot be achieved, the presence of fine α needles in the aged TLM and α-to-β transition are considered to play a crucial role in the subsequent nanostructuring.

IV. CONCLUSION

SMAT experiments performed on Ti–25Nb–2.9Mo–2Sn–3Zr indicated that the alloy undergoes a direct α-to-β structural phase transition at ambient temperature. SMAT not only results in phase transition but also refines the grains of the alloy. The phase transition first occurs at the α/β interfaces and then extends to the α phase interiors with increasing strain. It is irreversible in nature and diffusion controlled. The stress-induced increase of Gibbs energy and enrichment of Nb may cause a high order of lattice instability of the α phase adjacent to the α/β interfaces and compel the α phase to β phase. In the SMATed surface layer subjected to the most serious deformation, the α phase completely transforms to β phase. The presence of fine α needles in the aged alloy and the phase transition from α to β with increasing strain are viewed to play a crucial role in the subsequent nanostructuring.

ACKNOWLEDGMENTS

This work was financially supported by the National High Technology Research and Development Program of China (Grant 2006AA03Z0447) and the National Natural Science Foundation of China (Grants 50571079, 50671078).

REFERENCES

1. J.C. Jamieson: Crystal structures of titanium, zirconium, and hafnium at high pressures. *Science* **140,** 72 (1963).
2. D.R. Trinkle, R.G. Hennig, S.G. Srinivasan, D.M. Hatch, M.D. Jones, H.T. Stokes, R.C. Albers, and J.W. Wilkins: New mechanism for the alpha to omega martensitic transformation in pure titanium. *Phys. Rev. Lett.* **91,** 025701 (2003).
3. D. Errandonea, Y. Meng, M. Somayazulu, and D. Häusermann: Pressure-induced α→ω transition in titanium metal: A systematic study of the effects of uniaxial stress. *Physica B* **355,** 116 (2005).
4. A.K. Verma, P. Modak, R.S. Rao, B.K. Godwal, and R. Jeanloz: High-pressure phases of titanium: First-principles calculations. *Phys. Rev. B* **75,** 014109 (2007).
5. Y.K. Vohra and P.T. Spencer: Novel γ-phase of titanium metal at megabar pressures. *Phys. Rev. Lett.* **86,** 3068 (2001).
6. Y. Akahama, H. Kawamura, and T. Le Bihan: New δ (Distorted-bcc) titanium to 220 GPa. *Phys. Rev. Lett.* **87,** 275503 (2001).
7. R. Ahuja, L. Dubrovinsky, N. Dubrovinskaia, J.M.O. Guillen, M. Mattesini, B. Johansson, and T. Le Bihan: Titanium metal at high pressure: Synchrotron experiments and ab initio calculations. *Phys. Rev. B* **69,** 184102 (2004).
8. C.W. Greeff, D.R. Trinkle, and R.C. Albers: Shock-induced α–ω transition in titanium. *J. Appl. Phys.* **90,** 2221 (2001).
9. S.C. Gupta, K.D. Joshi, and S. Banerjee: Experimental and theoretical investigations on *d* and *f* electron systems under high pressure. *Metall. Mater. Trans. A* **39,** 1593 (2008).
10. Y. Ivanisenko, A. Kilmametov, H. Rosner, and R.Z. Valiev: Evidence of alpha→omega phase transition in titanium after high pressure torsion. *Int. J. Mater. Res.* **99,** 36 (2008).
11. M.T. Pérez-Prado, A.A. Gimazov, O.A. Ruano, M.E. Kassner, and A.P. Zhilyaev: Bulk nanocrystalline ω-Zr by high-pressure torsion. *Scr. Mater.* **58,** 219 (2008).
12. T. Saito, T. Furuta, J.H. Hwang, S. Kuramoto, K. Nishino, N. Suzuki, R. Chen, A. Yamada, K. Ito, Y. Seno, T. Nonaka, H. Ikehata, N. Nagasako, C. Iwamoto, Y. Ikuhara, and T. Sakuma: Multifunctional alloys obtained via a dislocation-free plastic deformation mechanism. *Science* **300,** 464 (2003).
13. J. Koike, Y. Shimoyama, I. Ohnuma, T. Okamura, R. Kainuma, K. Ishida, and K. Maruyama: Stress-induced phase transformation during superplastic deformation in two-phase Ti–Al–Fe alloy. *Acta Mater.* **48,** 2059 (2000).
14. Y.L. Hao, S.J. Li, S.Y. Sun, C.Y. Zheng, and R. Yang: Elastic deformation behaviour of Ti–24Nb–4Zr–7.9Sn for biomedical applications. *Acta Biomater.* **3,** 277 (2007).
15. N. Velisavljevic and G.N. Chesnut: Direct hcp → bcc structural phase transition observed in titanium alloy at high pressure. *Appl. Phys. Lett.* **91,** 101906 (2007).
16. H. Gleiter: Nanostructured materials: Basic concepts and microstructure. *Acta Mater.* **48,** 1 (2000).
17. L. Saldana, A. Méndez-Vilas, L. Jiang, M. Multigner, J.L. González-Carrasco, M.T. Pérez-Prado, M.L. González-Martín, L. Munuera, and N. Vilaboa: In vitro biocompatibility of an ultrafine grained zirconium. *Biomaterials* **28,** 4343 (2007).
18. D. Doraiswamy and S. Ankem: The effect of grain size and stability on ambient temperature tensile and creep deformation in metastable beta titanium alloys. *Acta Mater.* **51,** 1607 (2003).

19. L.C. Zhang, T. Zhou, S.P. Alpay, M. Aindow, and M.H. Wu: Origin of pseudoelastic behavior in Ti–Mo-based alloys. *Appl. Phys. Lett.* **87,** 241909 (2005).
20. W. Xu, K.B. Kim, J. Das, M. Calin, and J. Eckert: Phase stability and its effect on the deformation behavior of Ti–Nb–Ta–In/Cr β alloys. *Scr. Mater.* **54,** 1943 (2006).
21. W. Xu, K.B. Kim, J. Das, M. Calin, B. Rellinghaus, and J. Eckert: Deformation-induced nanostructuring in a Ti–Nb–Ta–In alloy. *Appl. Phys. Lett.* **89,** 031906 (2006).
22. Y.L. Hao, S.J. Li, S.Y. Sun, C.Y. Zheng, Q.M. Hu, and R. Yang: Super-elastic titanium alloy with unstable plastic deformation. *Appl. Phys. Lett.* **87,** 091906 (2005).
23. S.J. Li, T.C. Cui, Y.L. Li, Y.L. Hao, and R. Yang: Ultrafine-grained β-type titanium alloy with nonlinear elasticity and high ductility. *Appl. Phys. Lett.* **92,** 043128 (2008).
24. Z.T. Yu and L. Zhou: Influence of martensitic transformation on mechanical compatibility of biomedical β type titanium alloy TLM. *Mater. Sci. Eng., A* **438–440,** 391 (2006).
25. K. Lu and J. Lu: Nanostructured surface layer on metallic materials induced by surface mechanical attrition treatment. *Mater. Sci. Eng., A* **375–377,** 38 (2004).
26. G.W. Han, I.P. Jones, and R.E. Smallman: Direct evidence for Suzuki segregation and Cottrell pinning in MP159 superalloy obtained by FEG(S)TEM/EDX. *Acta Mater.* **51,** 2731 (2003).
27. K.Y. Zhu, A. Vassel, F. Brisset, K. Lu, and J. Lu: Nanostructure formation mechanism of α-titanium using SMAT. *Acta Mater.* **52,** 4101 (2004).
28. L. Zhang, Y. Han, and J. Lu: Nanocrystallization of zirconium subjected to surface mechanical attrition treatment. *Nanotechnology* **19,** 165706 (2008).
29. J.R. Spingarn and W.D. Nix: Diffusional creep and diffusionally accommodated grain rearrangement. *Acta Metall.* **26,** 1389 (1978).
30. R.M. Wentzcovitch: Hcp-to-bcc pressure-induced transition in Mg simulated by ab initio molecular dynamics. *Phys. Rev. B* **50,** 10358 (1994).